Article

Analytical Solutions of Water Inflow for Foundation Pit in Confined Water Stratum

Jingjing Shen [1], Yue Jiang [1], Jie Wu [2],* and Pengfei Li [2]

1   Beijing City Sub Central Station Integrated Hub Construction Management Co., Ltd., Beijing 100082, China
2   Key Laboratory of Urban Security and Disaster Engineering, Ministry of Education, Beijing University of Technology, Beijing 100124, China
*   Correspondence: wj@emails.bjut.edu.cn; Tel.: +86-18614024421

Abstract: This paper is aimed at the problem of inaccurate calculation of the water inflow of a foundation pit with a suspended water-proof curtain in a confined water stratum. According to the groundwater hydraulics principle, the theoretical model of the seepage field of the foundation pit is established, and the analytical formula of the water inflow for the circular, strip, and rectangular foundation pits is deduced. The seepage path influence coefficient α related to the water-proof curtain insertion ratio, the thickness of the confined aquifer, and the radius of the foundation pit is proposed and obtained by the positive and negative analysis of numerical simulation. The coefficient is used to correct the equivalent seepage length in the pit and directly affect the calculation result of water inflow. Finally, based on the calculation results of the analytical solution of water inflow, the relationship between the scale of the foundation pit and the water control effect is discussed. The research results show that the theoretical analysis results in this paper are in good agreement with the numerical results and the measured data in the field: when the size of the foundation pit is too large, it is not suitable to use the suspended water-proof curtain as the water control measure.

Keywords: foundation pit; seepage fields; water-proof curtain; seepage path influence coefficient

1. Introduction

In recent years, with the continuous improvements in national economies and urbanization levels, more and more high-rise buildings and large-scale underground structures have appeared in cities, resulting in the number of deep foundation pits sharply increasing [1–4]. However, the deep foundation pit often encounters the confined water stratum during the excavation process, and dewatering measures need to be taken to avoid problems such as groundwater inrushing and overall floating when the hydraulic head is high [5,6]. Among the existing dewatering measures, the "wall–well" dewatering system [7–9], which is composed of pumping wells and suspended water-proof curtains, has been widely used because of the advantages of outstanding water control effect and economic benefits. During the design of the "wall–well" system, it is necessary to accurately calculate the water inflow to reasonably determine the dewatering capacity [10–12]. Extensive existing research has studied the water inflow of the foundation pits with suspended water-proof curtains from analytical solutions, numerical simulation, and site measurements. Shen [13] considered the barrier effect of the water-proof curtain from two cases and proposed a series of simple equations to calculate the head difference at the two sides of the water-proof curtain. Wang [14] carried out the numerical simulation of the large deep excavation by 3D finite difference method (FDM) and compared it with the observation results; the analysis results show that the water-proof curtain can minimize seepage and uplift in large excavation pits, although settlement outside the pit may need treatment measures. Pujades [15] used numerical and analytical methods to derive semi-empirical equations to quantify the two barrier effects for semi-permeable, partially penetrating (or fully penetrating but finite in length), and barriers with a by-pass in confined aquifers, obtaining excellent agreement

between the calculated and observed barrier effects at two construction sites. Wu [16] investigated the mechanism of the blocking effect, which is affected by dewatering through the finite difference method; the results show that drawdown varies along the depth of the confined aquifer, and the influence factors of drawdown inside and outside the pit include insertion depth of retaining walls, anisotropy of a confined aquifer, and screen length of pumping wells. Luo [17] conducted a three-dimensional finite element simulation to analyze the dewatering process of the Dongjiadu subway tunnel repair foundation pit in Shanghai. Li [18] regarded the foundation pits with suspended water-proof curtains as a large-diameter vertical well, and a simplified formula for water inflow calculation of foundation pit dewatering was derived; the simplified formula had a higher accuracy when the curtain insertion ratio was greater than 0.6 and the value of the foundation pit radius to confined aquifer thickness was less than 2.0.

In conclusion, the existing analytical solutions do not have a good consistency with numerical solutions and site-measured values. They only have good accuracy in some specific r_0/M and L/M intervals (where r_0 is the radius of the circular foundation pit, L is the insertion depth of the water-proof curtain, and M is the thickness of the confined aquifer). The reason is that the equivalent length of the seepage path applied in water inflow calculation is unreasonable. Numerical methods are based on specific engineering projects, and the accuracy of the results depends on the selection of parameters and boundary conditions [8–11,14], which is not universal. This paper obtained the analytical solutions of water inflow for multi-shape foundation pits, introduced the influence coefficient α of seepage path length, and proposed the expressed formula. The results show that the analytical solutions in this paper are in good agreement with the numerical results and measured data.

2. Water Inflow Solutions of Circular and Strip Foundation Pits

Only radial seepage is considered; the seepage analytical models of strip foundation pits and circular foundation pits can be regarded as two-dimensional cases. The central axis of the foundation pit is taken as the z-axis, the radial direction of the foundation pit is taken as the r-axis, and the intersection of the central axis and the bottom plate of the aquifer is selected as the origin to establish a coordinate system. The central axis and the radial direction of the foundation pit are taken as the z-axis and the r-axis, respectively. A coordinate system is established in which the origin is the intersection of the central axis and the bottom of the aquifer. According to the principle of hydraulics, the theoretical model of the foundation pit with the suspended water-proof curtain in the confined water stratum is established. As shown in Figure 1, where H is the water table of the confined water, r_0 is the length from the central axis of the foundation pit to the excavation boundary, R is the influence radius of dewatering, h_0 is the value of the hydraulic contour line at the bottom of the water-proof curtain, $D(z)$ is the hydraulic head distribution function on the outer side of the water-proof curtain, H_d is the water table in the foundation pit, H_w is the hydraulic head at the maximum drawdown position of the aquifer, L is the length of the water-proof curtain inserted into the aquifer, and M is the thickness of the aquifer.

To obtain water inflow of the foundation pit in a confined water stratum, several assumptions are made: the thickness of the water-proof curtain is ignored; there is a steady seepage process in the calculation region; the water table in the foundation pit is horizontal; only radial seepage is considered The seepage region can be divided into three parts: the outside of the foundation pit (Region 1), the region below the water-proof curtain in the foundation pit (Region 2), and the vertical seepage region in the pit (Region 3). Due to the water interception effect of the water-proof curtain, the water in Region 1 flows around into Region 2, and the water horizontally flows below the water-proof curtain, then the flow direction is turned in Region 2 and the water flows into Region 3 vertically.
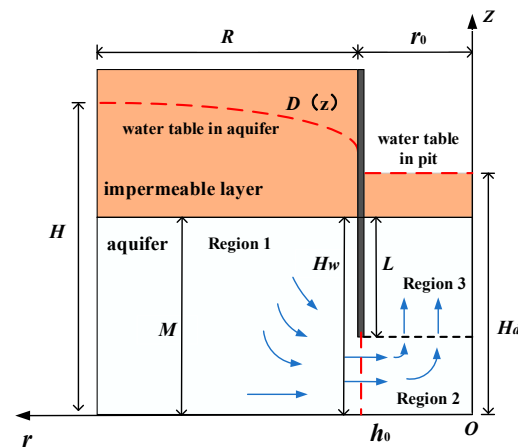
Figure 1. Theoretical model for pit with suspended water-proof curtain in confined water stratum.

Based on the seepage continuity, the water inflow in the three regions is the same, namely:

$$Q_1 = Q_2 = Q_3 = Q \tag{1}$$

where Q_1, Q_2, and Q_3 are the water inflow in the three regions, respectively; Q is the water inflow in the foundation pit. Because only radial seepage is considered, the hydraulic head distribution in the seepage region is independent of the angle, based on the two-dimensional condition, the hydraulic head at each point in the seepage region can be expressed as $h(r, z)$, and the boundary conditions in the seepage region are given as:

$$\begin{cases} h(r,z) = H; \ r = r_0 + R, \ z > 0 \\ \frac{\partial h(r,z)}{\partial z} = 0; \ 0 \leq r \leq r_0 + R, \ z = 0 \\ \frac{\partial h(r,z)}{\partial z} = 0; \ r_0 < r \leq r_0 + R, \ z = M \\ h = h_0; \ r = r_0, \ 0 \leq z \leq M - L \\ h = D(z); \ r = r_0, \ M - L \leq z \leq M \\ h(r,z) = H_d; \ 0 < r < r_0, \ z = H_d \end{cases} \tag{2}$$

2.1. Water Inflow Calculation Outside the Foundation Pit

According to Darcy's law, the horizontal seepage velocity for each point in the aquifer can be calculated as:

$$v_r = -k_r \frac{\partial h(r,z)}{\partial r} \tag{3}$$

where v_r is the horizontal seepage velocity and k_r is the horizontal permeability coefficient in the confined aquifer. The flow rate through each section in Region 1 can be expressed as:

$$Q_1 = -2\pi r \int_0^M v_r dz \tag{4}$$

Substituting Equation (3) into Equation (4), water inflow for the circular and strip foundation pit in Region 1 can be denoted as:

$$\begin{aligned} Q_1 &= 2\pi r k_r \int_0^M \frac{\partial h(r,z)}{\partial r} dz \\ Q_1 &= l k_r \int_0^M \frac{\partial h(r,z)}{\partial r} dz \end{aligned} \tag{5}$$

where l is the length of the strip pit. According to the existing experimental and field monitoring data [19–22], the distribution law of hydraulic head on the outer side of the water-proof curtain can be approximated as:

$$D(z) = \sqrt{\frac{z - M + L}{L}} (H_w - h_0) + h_0 \tag{6}$$

by substituting boundary conditions Equations (2) and (6) into Equation (5), the water inflow outside the circular and strip foundation pit can be calculated as:

$$Q_1 = \frac{2\pi k_r[3M(h_0 - H) + 2L(H_w - h_0)]}{3\ln\frac{r_0}{R + r_0}}$$
$$Q_1 = \frac{lk_r[3M(h_0 - H) + 2L(H_w - h_0)]}{R} \tag{7}$$

2.2. Water Inflow Calculation in the Foundation Pit

The water in Region 1 flows around into Region 2, then the flow direction is turned in Region 2 and there is only water flowing vertically in Region 3. Therefore, the shortest seepage path $L_{\min}$ of water flow in Region 2 and Region 3 is denoted by:

$$L_{\min} = H_d - M + L \tag{8}$$

The longest seepage path $L_{\max}$ is:

$$L_{\max} = r_0 + H_d \tag{9}$$

It should be pointed out that if the hydraulic head is in the impermeable layer, that is, $H_d > M$, then H_d in Equations (8) and (9) is replaced by M. When Darcy's law is used to calculate the water inflow in the foundation pit, most of the existing analytical solutions are to replace the equivalent seepage length by the average of the longest seepage path and the shortest seepage path [13,18], or $2L_{\min}$. The water inflow calculated by those two methods is only reasonable in the specific intervals of r_0/M and L/M. In fact, the length of the equivalent seepage path that is used to calculate the water inflow in the foundation pit should vary with r_0/M and L/M, and it is unreasonable to substitute by $(L_{\max} + L_{\min})/2$ or $2L_{\min}$. In order to accurately calculate the water inflow in the foundation pit in the confined water stratum, the seepage path influence coefficient α, which can reflect the change in the equivalent seepage path length with r_0/M and L/M, is introduced, and the fitting formula is explored through numerical simulation in the next section. The length of the equivalent seepage path can be expressed as:

$$\overline{L} = \alpha \cdot \frac{(L_{\max} + L_{\min})}{2} = \frac{\alpha(2H_d + r_0 - M + L)}{2} \tag{10}$$

where α is the function whose variables are r_0/M and L/M:

$$\alpha = f\left(\frac{r_0}{M}, \frac{L}{M}\right) \tag{11}$$

The water inflow for the circular and strip foundation pit in Region 2 and Region 3 is calculated by:

$$Q_2 = Q_3 = k_v \frac{2\pi r_0^2(h_0 - H_d)}{\alpha(2H_d + r_0 - M + L)}$$
$$Q_2 = Q_3 = k_v \frac{lr_0(h_0 - H_d)}{\alpha(2H_d + r_0 - M + L)} \tag{12}$$

where k_v is the vertical permeability coefficient.

2.3. The Hydraulic Head at the Maximum Drawdown Position of the Aquifer H_w

Under the condition of ignoring the thickness of the water-proof curtain, the reduction of hydraulic head is greater than the outer side of the curtain when the water flows through the inner side of the curtain. Based on the existing experimental and field monitoring data [19–22], the reduction of the hydraulic head when the water flows through the inner side of the curtain accounts for about 2/3 of the total reduction in the unconfined aquifer. However, the direction and characteristics are the same whether the water flows around

the water-proof curtain in the confined water stratum or the unconfined water stratum. The conclusion applied to the confined water case can be expressed as:

$$h_0 = H_d + \frac{2}{3}(H_w - H_d) \tag{13}$$

Based on the principle of seepage continuity and combining Equations (7), (12), and (13), the hydraulic head at the maximum drawdown position of the aquifer H_w for the circular foundation pits can be expressed as:

$$H_w = \frac{H_d\left[k_r(3M - 2L) + \left(\frac{6r_0^2 k_v \ln \frac{r_0}{R + r_0}}{\alpha(2H_d + r_0 - M + L)}\right)\right] - 9k_r MH}{\frac{6r_0^2 k_v \ln \frac{r_0}{R + r_0}}{\alpha(2H_d + r_0 - M + L)} - 2k_r(3M + L)} \tag{14}$$

To substitute Equations (13) and (14) into Equation (12), the water inflow in the foundation pit can be obtained.

2.4. The Influence Coefficient α of Seepage Path in Confined Water Stratum

To investigate characteristics of the seepage path influence coefficient α, a seepage numerical model for the circular foundation pits is established. Based on the symmetry, a quarter of the model is set to increase calculation efficiency, which is shown in Figure 2. The stratum conditions of the numerical model are sandy–sticky mixed stratum, and the aquifer is mainly fine sand, where the permeability coefficient is $k_r = k_v = 5 \times 10^{-6}$ m/s, the hydraulic head for the confined water aquifer is $H = 30$ m, the hydraulic head in the foundation pit is $H_d = 30$ m, and the thickness of the aquifer is $M = 10$ m. The radial boundary of the model is a fixed hydraulic head, the excavation surface of the foundation pit is the free boundary, and the pore water pressure 0 is fixed. The water-proof curtain and the impermeable layer are impermeable boundaries; the other boundaries are fixed by the normal seepage velocity.
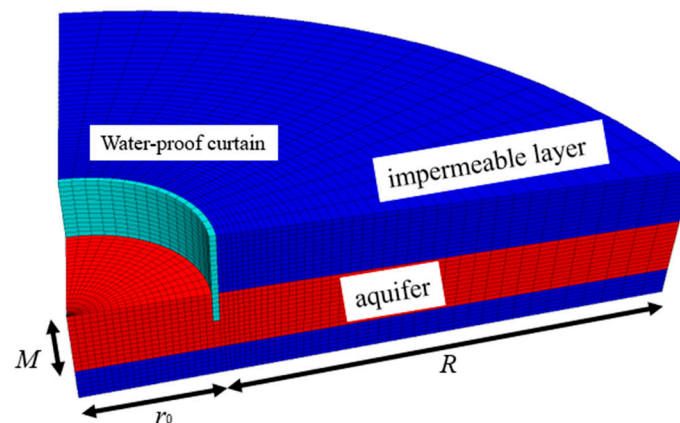

Figure 2. Numerical model for the pit with suspended water-proof curtain in confined water stratum.

r_0/M = 1, 3, 5, 7, 9 are selected as the test cases and to explore the variation in the coefficient α. The remaining conditions are selected as the verification cases. Figure 3 shows the variation in water inflow with r_0/M and L/M. It can be seen from Figure 3a that L/M has a greater impact on water inflow than r_0/M. The water inflow in the foundation pit decreases as L/M increases, and when the scale of the foundation pit is small ($r_0/M = 1$), the water inflow has the linear relationship with L/M. However, in other cases, the water inflow initially decreases linearly as L/M increases, then decreases exponentially. Under the same value of L/M, as r_0/M increases, the water inflow continues to increase, but the increase rate decreases. The variation in the influence coefficient α with r_0/M and L/M are shown in Figure 4. It can be seen from Figure 3a that both the r_0/M and L/M have a
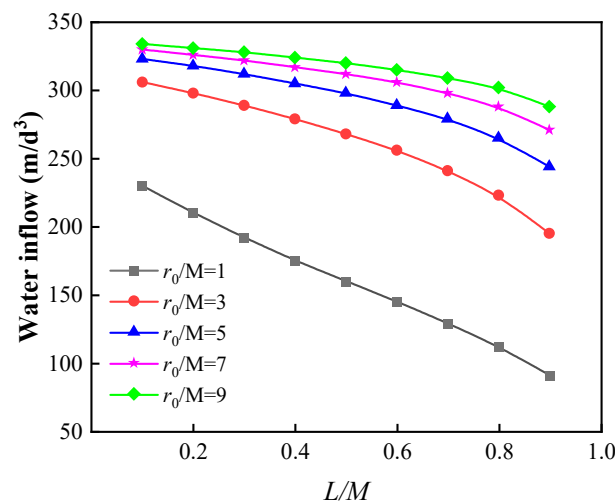
significantly effect on α. What is more, L/M has a greater influence. If the effect of L/M on the equivalent seepage path is ignored, that is, taking α equal to 1, the analytical solution of water inflow is consistent with the numerical results when L/M is 0.7~0.8 in Figure 4a. As L/M increases, α firstly increases linearly, and then increases exponentially, approximately with $L/M = 0.7$ as the critical point. As r_0/M increases, α firstly increases and then decreases, and the inflection point is $r_0/M = 3$. It can be seen from Figure 4b that $r_0/M = 3$ is the dividing point of the trend of influence coefficient. This is because, when $r_0/M < 3$, the seepage direction of water in the foundation pit is close to the vertical direction, and the equivalent seepage path is close to the shortest seepage path $L_{\min}$. Under the same L/M, the smaller the r_0/M, the smaller the coefficient α. According to the characteristics of α in Figure 4a, the functional relationship between α and L/M is established as follows:

$$\alpha = \begin{cases} A + K\left(\frac{L}{M}\right) & (0 < L/M < 0.7) \\ I + B_1\left(\frac{L}{M}\right) + B_2\left(\frac{L}{M}\right)^2 & (0.7 \le L/M < 1) \end{cases} \tag{15}$$

where A is the intercept of the linear function; K is the slope of the linear function; I is the intercept of the quadratic polynomial; B_1 is the coefficient of the linear term; B_2 is the coefficient of a quadratic term. Fitting Equation (15) with the curve in Figure 4a obtains parameters A, K, I, B_1, and B_2 under different r_0/M. Then, the functional relationship between r_0/M and those parameters is established as follows:
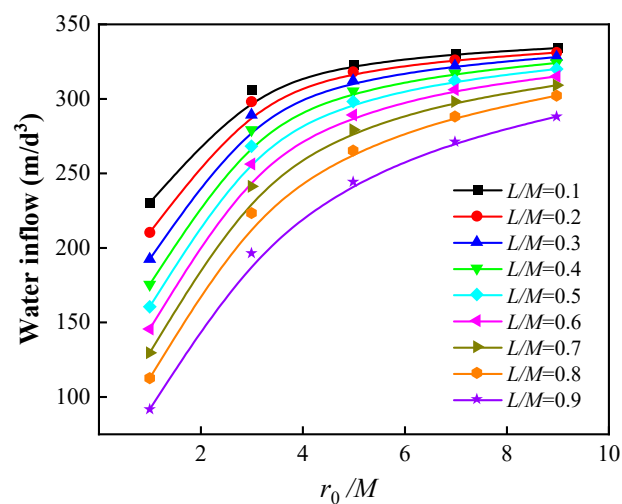
$$\begin{cases} A = a_1 + a_2\left(\frac{r_0}{M}\right) \\ K = k_1 + k_2\left(\frac{r_0}{M}\right) \\ I = i_1 + i_2\left(\frac{r_0}{M}\right) \\ B_1 = b_1 + b_2\left(\frac{r_0}{M}\right) \\ B_2 = b_3 + b_4\left(\frac{r_0}{M}\right) \end{cases} \tag{16}$$

where a_1, a_2, k_1, k_2, i_1, i_2, b_1, b_2, b_3, and b_4 are all the terms of the linear function parameter.
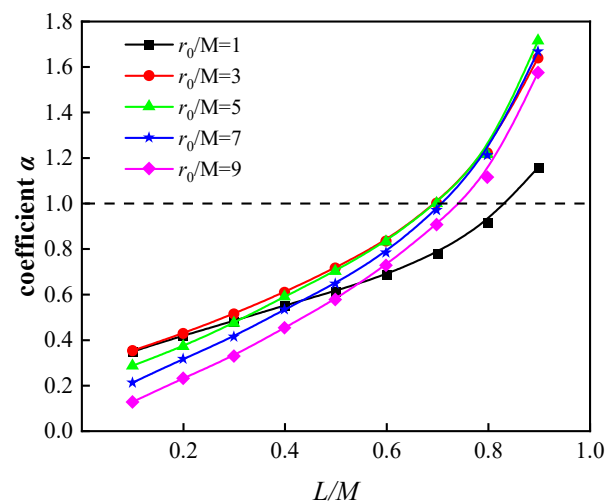

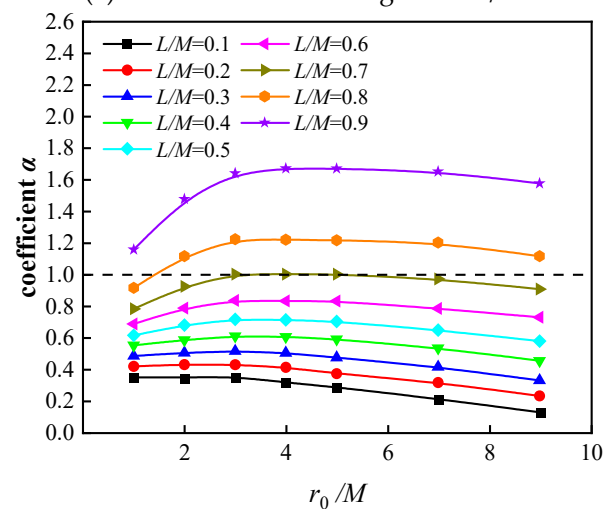(**a**) The water inflow change with L/M.

Figure 3. *Cont.*

(**b**) The water inflow change with r_0/M.

Figure 3. The variation in water inflow with the change in r_0/M and insertion ratio of curtain.

(**a**) The coefficient α change with L/M.

(**b**) The coefficient α change with r_0/M.

Figure 4. The variation in α with the change in r_0/M and insertion ratio of curtain.

Substituting the A, K, I, B_1, and B_2 under different r_0/M into Equation (16), the terms of the linear function can be solved. And the seepage path influence coefficient α can be expressed as:

$$
\alpha \begin{cases} 0 < r_0/M \le 3 \begin{cases} 0.3 - 0.02\left(\frac{r_0}{M}\right) + \left[0.53 + 0.15\left(\frac{r_0}{M}\right)\right]\left(\frac{L}{M}\right) \ (0 < L/M < 0.7) \\ 1.9 + \left(\frac{r_0}{M}\right) - \left[4.1 + 2.83\left(\frac{r_0}{M}\right)\right]\left(\frac{L}{M}\right) \\ \quad + \left[3.33 + 2.18\left(\frac{r_0}{M}\right)\right]\left(\frac{L}{M}\right)^2 \quad (0.7 \le L/M < 1) \end{cases} \\ r_0/M > 3 \begin{cases} 0.35 - 0.04\left(\frac{r_0}{M}\right) + \left[1 + 0.02\left(\frac{r_0}{M}\right)\right]\left(\frac{L}{M}\right) \ (0 < L/M < 0.7) \\ 1.62 + 0.55\left(\frac{r_0}{M}\right) - \left[4 + 1.4\left(\frac{r_0}{M}\right)\right]\left(\frac{L}{M}\right) \\ \quad + \left[4.8 + 0.85\left(\frac{r_0}{M}\right)\right]\left(\frac{L}{M}\right)^2 \quad (0.7 \le L/M < 1) \end{cases} \end{cases}
\tag{17}
$$

3. Analysis of Water Inflow for the Rectangular Foundation Pits

In engineering projects, the shape of most foundation pits can be approximately regarded as a rectangle. However, for convenience, the foundation pit is equivalent to the circle according to the principle of the same area, then the water inflow is calculated by the analytical solutions which are suitable for the circular foundation pit. In order to explore the variance of water inflow for different size characteristics of rectangular foundation pits in confined water stratum, the numerical simulation is used to calculate the water inflow under different length-to-width ratios ρ based on the condition that the total area is equal. The circular foundation pit with a diameter of 20 m is selected as a criterion. The rectangular foundation pits' models are established with the length-to-width ratios ρ = 1:1, 2:1, 3:1, 5:1, and 9:1 based on the condition of equal total areas. The soil parameters and boundary conditions are the same as the above. In addition, the models of strip foundation pits with widths of 6 m and 8 m were established, respectively. Figure 5 shows the variation in water inflow with L/M for different shapes of foundation pits. It can be seen from the figure that the variation in water inflow with L/M for different shapes of foundation pits have the same trend. However, the shape characteristic has a great effect on the water inflow. Under the condition that the foundation pit area is equal, the water inflow of the strip foundation pit is much larger than that of the circular foundation pit with the same L/M, the former is about twice as much as the latter when L/M = 1. The water inflow of the square foundation pit (i.e., the length-to-width ratio is 1) is the same as the circular foundation pit; the more difference between length and width, the more difference between water inflow. When the length-to-width ratio is 2, the water inflow of the rectangular foundation pits under each curtain insertion ratio is slightly larger than that of the circular foundation pits, but the difference between them is not large and the maximum difference is less than 5%, which is within the acceptable range. Therefore, the water inflow calculation formula of the circular foundation pit can still be used in that case. When the length-to-width ratio ρ = 5, 9, the water inflow of the rectangular foundation pits is basically the same as the strip foundation pits under the same L/M. Therefore, for the calculation of water inflow, the rectangular foundation pits where the length-to-width ratio is greater than 5 can be regarded as strip foundation pits. When the length-to-width ratio is 3 or 4, the water inflow in that two cases is basically the same, but they are much larger than that of the circular foundation pit and much smaller than that of the strip foundation pit under the condition of equal area. The water inflow for the rectangular foundation when the length-to-width ratio is 3 or 4 can be calculated as the average value of the water inflow of the circular foundation pit and the rectangular foundation pit with a length-to-width ratio of ρ = 5.
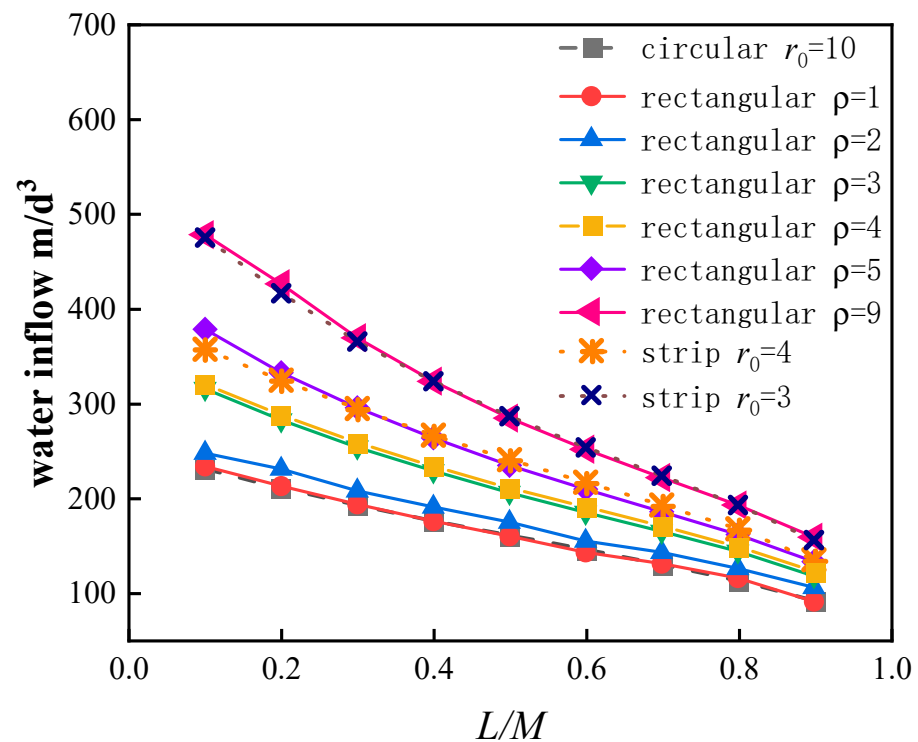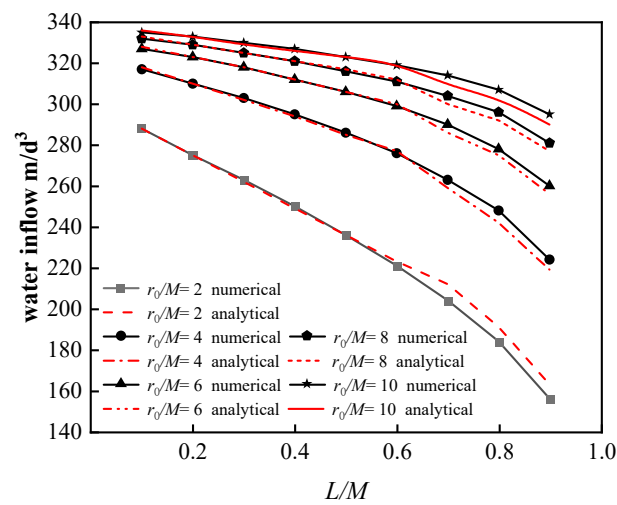
Figure 5. The variation in water inflow with the change of L/M for different shapes of foundation pits.
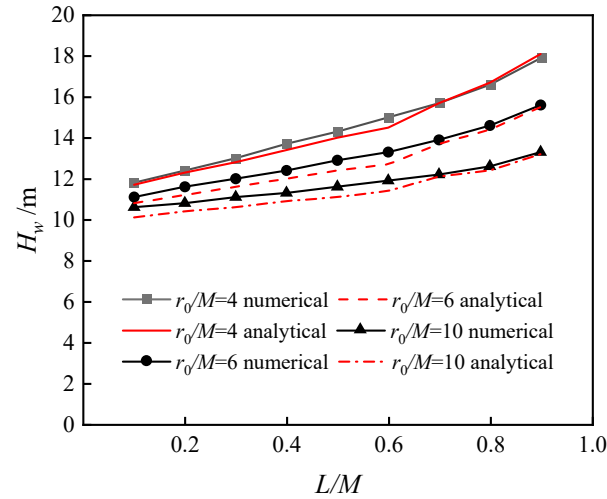
4. Verification and Analysis

4.1. Supplementary Cases Verification

The water inflow of the circular foundation pit under different cases is chosen for verification and analysis. Figure 6a shows the comparison between the analytical solution and numerical solution calculation results of water inflow under verification cases. From Figure 6a, it can be seen that the water inflow decreases nonlinearly as the L/M increases and the analytical solutions are consistent with the numerical simulations. The maximum RMSE of the two results is 4.18. Figure 6b shows the comparison between the two results of H_w under the cases of $r_0/M = 4$, 6, and 10. It can be seen from the figure that the two results have the same trend and H_w increases nonlinearly as the L/M increases. When $L/M > 0.7$, the H_w obtained by the two methods is basically the same. When $0 < L/M < 0.7$, the analytical solutions are slightly smaller than the numerical solutions. The maximum RMSE of the two results is 3.32.

In order to verify the universality of the derived solutions, several parameters include the soil permeability coefficient k, confined aquifer thickness M, and the difference in hydraulic head $H-H_d$ are changed, and the water inflow under changed parameters are calculated. Figure 7 shows the water inflow of the analytical solutions and numerical results under changed parameters. The figure shows that the water inflow decreases nonlinearly as the L/M increases under all changed parameters. The water inflow increases with the increase in the soil permeability coefficient k, confined aquifer thickness M, and the difference in hydraulic head $H-H_d$, respectively.
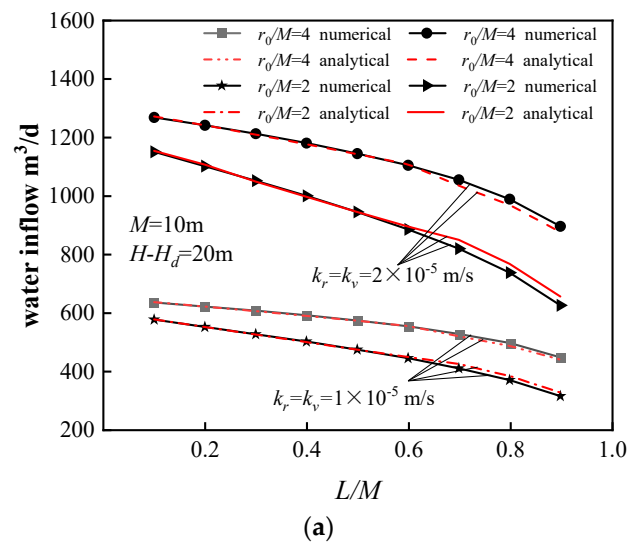
(**a**) The variation in water inflow with *L/M*.

(**b**) The variation in H_w with *L/M*.

Figure 6. Water inflow and H_w in different cases of foundation pit.

(**a**)

Figure 7. *Cont.*
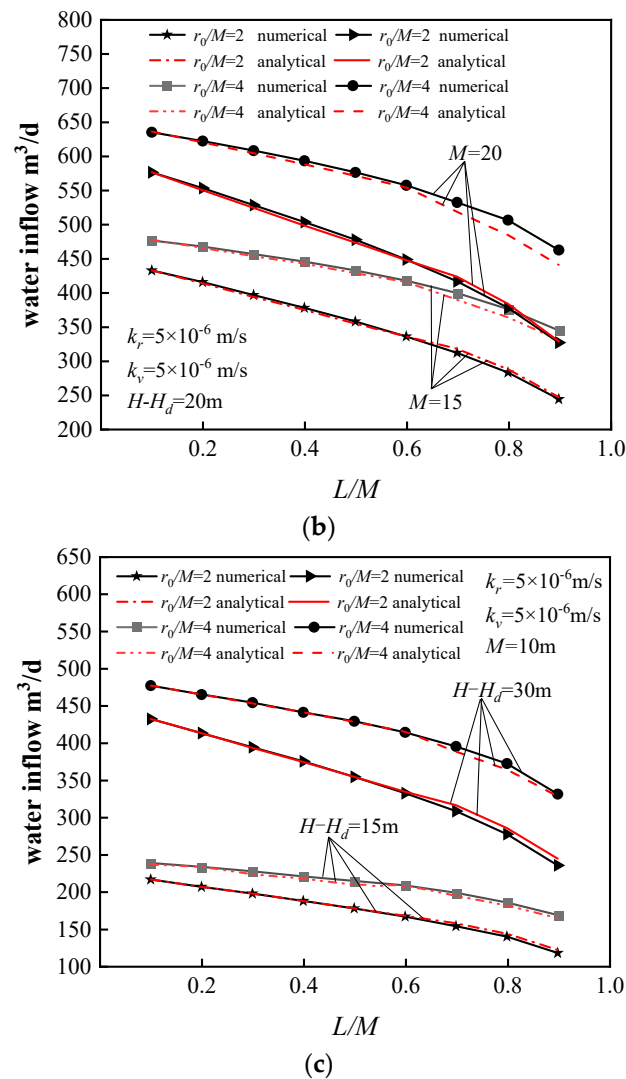
(**b**)

(**c**)

Figure 7. Parameter sensitivity analysis. (**a**) The variation in water inflow with L/M for different permeability coefficients; (**b**) the variation in water inflow with L/M for different thickness of aquifer; (**c**) the variation in water inflow with L/M for different hydraulic heads.

4.2. Comparison and Analysis between Analytical Solution and Site Measured Data

Table 1 shows the comparison result of water inflow between the analytical solution and the actual measured values in the project. Q_{c1} and Q_r in Table 1 are the water inflow of the analytical solution and the measured values at the site from the reference [18], respectively. It is pointed out that Q_{c1} does not consider the influence coefficient α. Q_{c2} refers to the analytical solutions in this paper. Q_j is the water inflow calculated by the formula from the specification [23], which does not consider the influence of the water-proof curtain. It can be seen from Table 1 that both Q_{c1} and Q_{c2} are much smaller than Q_j. This shows that a water-proof curtain can effectively reduce the water inflow in foundation pits. It can be known from the comparison of Q_{c1} and Q_{c2} that Q_{c2} is much closer to the measured value than Q_{c1}. Indicating that the influence coefficient α has a great impact on the calculation of water inflow, and the calculation results considering the influence coefficient α are more accurate. Q_{c2} is slightly larger than the measured value; it is safer for water inflow calculation in actual dewatering projects.

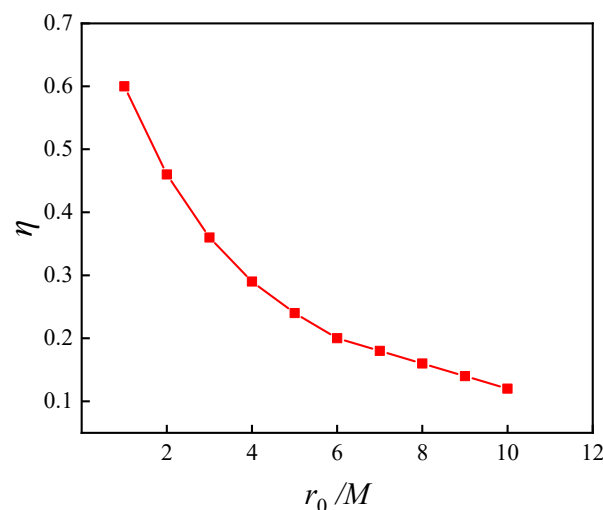**Table 1.** Comparison of analytical solution and measured values.

Projects	Parameters of the Foundation Pits										Q_{c1} /(m³/day)	Q_{c2} /(m³/day)	Q_r /(m³/day)	Q_j /(m³/day)
	M /m	k_v /(m³/day)	k_r/k_v	R /m	H /m	H_d /m	L /m	r_0 /m	L/M	r_0/M				
1	25	17.3	5	900	48	32	4	10	0.16	0.40	8190	6900	6000	38,540
2	32	17.3	5	900	52	34	9	10	0.28	0.31	4830	5058	4440	50,145
3	35	17.3	5	900	51	39	31	31	0.89	0.89	8839	7680	7200	55,417
4	35	17.3	5	900	51	39	31	26	0.89	0.75	6493	5972	4800	52,231

4.3. The Water Control Effect Analysis

The analysis of water inflow from Figures 3 and 6 reveals that when L/M is constant, the water inflow rises with an increase in r_0/M. However, the rate of increase in water inflow slows significantly, and the variation in water inflow with L/M becomes less apparent. We are defining the Q_{i1} and Q_{i9} as the water inflow corresponding to $L/M = 0.1$ and $L/M = 0.9$, respectively. η is denoted as:
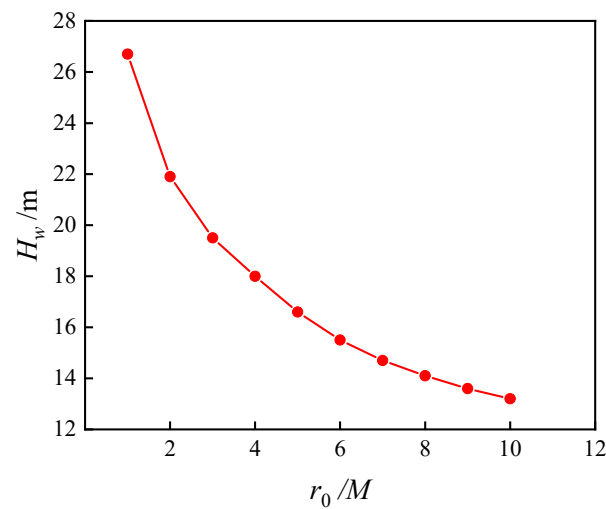
$$\eta = \frac{Q_{i1} - Q_{i9}}{Q_{i1}} \tag{18}$$

where η can reflect the water blocking effect of water-proof curtains under different sizes of foundation pits: the larger the value, the better the water blocking effect. It can be seen from Figure 8a that the water blocking effect gradually decreases with the increase in r_0/M. When $0 < r_0/M < 5$, the water blocking effect decreases significantly with the increase in r_0/M. After $r_0/M > 5$, the value of η has been much smaller than the initial value and no longer changes obviously. Figure 8b shows the relationship between H_w and r_0/M when the insertion ratio is large ($L/M = 0.9$). The smaller H_w is, the greater impact of dewatering on the confined water table outside the pit. As r_0/M increases, the impact of dewatering on the confined water table increases. After $r_0/M > 5$, the value of H_w has been much smaller than the initial hydraulic head outside the pit ($H = 30$ m) and no longer changes obviously. Considering the water blocking effect (the degree of water inflow reduction with the increase in L/M) and the protection of water resources (the impact of dewatering on the water table outside the pit), when the size of the foundation pit is large, the water-proof curtain should insert to the bottom of the aquifer that cuts off the hydraulic connection between the inside and outside of the foundation pit.

(**a**) The variation in η with r_0/M.

Figure 8. *Cont.*

(**b**) The variation in H_w with r_0/M.

Figure 8. The variation in water blocking effect with r_0/M.

5. Conclusions

This paper introduces a calculation model for water inflow in foundation pits with suspended waterproof curtains in confined water strata. Analytical solutions for water inflow in circular, strip, and rectangular foundation pits are derived. The calculation formula of the seepage path influence coefficient α is derived by fitting with the numerical results. By comparing with a large number of numerical results of supplementary cases and site measured data, the correctness and universality of the analytical solutions in this paper are verified:

(1) For the solutions of the water inflow in the foundation pit for the foundation pit with the suspended water-proof curtain in the confined water stratum, the seepage path influence coefficient α has a great impact on the calculation results, and it should be determined by the scale of the foundation, the thickness of the aquifer, and the insertion ratio of the curtain;

(2) The ratio of the foundation pit radius to the thickness of the aquifer (r_0/M) and the insertion ratio of the curtain (L/M) have a significant influence on the seepage path influence coefficient α, and the dividing points of their influence are $r_0/M = 3$ and $L/M = 0.7$, respectively;

(3) For the water inflow calculation of the rectangular foundation pit, when the length-to-width ratio is greater than 1 and less than 2, the rectangular foundation pit is equivalent to a circular foundation pit according to the principle of equal areas, when the length-to-width ratio is greater than 5, the rectangular foundation pit is equivalent to a strip foundation pit according to the principle of equal areas, and interpolation should be adopted in other cases;

(4) When the suspended water-proof curtain is selected as the measure to control the groundwater, the water control effect will decrease with the increase in r_0/M. When the size of the foundation pit is large, the curtain should be inserted into the bottom of the aquifer to cut off the hydraulic connection between the inside and outside of the foundation pit.

Author Contributions: Conceptualization, J.W. and J.S.; methodology, J.W. and Y.J.; software, J.W.; Writing—review & editing: J.S. and Y.J.; Project administration: J.S. and Y.J.; Supervision: P.L. All authors have read and agreed to the published version of the manuscript.

Data Availability Statement: Data will be made available on request.

Conflicts of Interest: Authors Jingjing Shen and Yue Jiang were employed by the company Beijing City Sub Central Station Integrated Hub Construction Management Co., Ltd. The remaining authors declare that the research was conducted in the absence of any commercial or financial relationships that could be construed as a potential conflict of interest.

References

1. Chai, J.-C.; Shen, S.-L.; Zhu, H.-H.; Zhang, X.-L. Land subsidence due to groundwater drawdown in Shanghai. *Géotechnique* **2004**, *54*, 143–147. [CrossRef]
2. Wan, T.; Li, P.; Zheng, H.; Zhang, M. An analytical model of loosening earth pressure in front of tunnel face for deep-buried shield tunnels in sand. *Comput. Geotech.* **2019**, *115*, 103170. [CrossRef]
3. Xue, Y.; Zhou, B.; Ge, S.; Qiu, D.; Gong, H. Optimum design calculation method for the reasonable buried depth: A case study from Hong Kong-Zhuhai-Macao immersed tunnel. *Ocean. Eng.* **2020**, *206*, 107275. [CrossRef]
4. Font-Capó, J.; Vázquez-Suñé, E.; Carrera, J.; Martí, D.; Carbonell, R.; Pérez-Estaun, A. Groundwater inflow prediction in urban tunneling with a tunnel boring machine (TBM). *Eng. Geol.* **2011**, *121*, 46–54. [CrossRef]
5. Xu, Y.-S.; Ma, L.; Shen, S.-L.; Sun, W.-J. Evaluation of land subsidence by considering underground structures that penetrate the aquifers of Shanghai, China. *Hydrogeol. J.* **2012**, *20*, 1623–1634. [CrossRef]
6. Wang, Y.; Jiao, J.J. Origin of groundwater salinity and hydrogeochemical processes in the confined Quaternary aquifer of the Pearl River Delta, China. *J. Hydrol.* **2012**, *438–439*, 112–124. [CrossRef]
7. Wu, Y.-X.; Shen, S.-L.; Wu, H.-N.; Xu, Y.-S.; Yin, Z.-Y.; Sun, W.-J. Environmental protection using dewatering technology in a deep confined aquifer beneath a shallow aquifer. *Eng. Geol.* **2015**, *196*, 59–70. [CrossRef]
8. Wang, J.-X.; Feng, B.; Liu, Y.; Wu, L.-G.; Zhu, Y.-F.; Zhang, X.-S.; Tang, Y.; Yang, P. Controlling subsidence caused by de-watering in a deep foundation pit. *B Eng. Geol. Environ.* **2012**, *71*, 545–555. [CrossRef]
9. Pujades, E.; Vázquez-Suñé, E.; Carrera, J.; Vilarrasa, V.; De Simone, S.; Jurado, A.; Ledesma, A.; Ramos, G.; Lloret, A. Deep enclosures versus pumping to reduce settlements during shaft excavations. *Eng. Geol.* **2014**, *169*, 100–111. [CrossRef]
10. Pujades, E.; Vàzquez-Suñé, E.; Carrera, J.; Jarado, A. Dewatering of a deep excavation undertaken in a layered soil. *Eng. Geol.* **2014**, *2014*, 15–27. [CrossRef]
11. Ma, L.; Xu, Y.-S.; Shen, S.-L.; Sun, W.-J. Evaluation of the hydraulic conductivity of aquifer with piles. *Hydrogeol. J.* **2014**, *22*, 371–382. [CrossRef]
12. Zeng, C.F.; Song, W.W.; Xue, X.L.; Li, M.K.; Bai, N.; Mei, G.X. Construction dewatering in a metro station incorporating buttress retaining wall to limit ground settlement: Insights from experimental modelling. *Tunn. Undergr. Space Technol.* **2021**, *116*, 104124. [CrossRef]
13. Shen, S.-L.; Wu, Y.-X.; Misra, A. Calculation of head difference at two sides of a cut-off barrier during excavation dewatering. *Comput. Geotech.* **2017**, *91*, 192–202. [CrossRef]
14. Wang, J.-X.; Feng, B.; Yu, H.; Guo, T.-P.; Yang, G.-Y.; Tang, J.-W. Numerical study of dewatering in a large deep foundation pit. *Environ. Earth Sci.* **2013**, *69*, 863–872. [CrossRef]
15. Pujades, E.; López, A.; Carrera, J.; Vázquez-Suñé, E.; Jurado, A. Barrier effect of underground structures on aquifers. *Eng. Geol.* **2012**, *2012*, 41–49. [CrossRef]
16. Wu, Y.-X.; Shen, S.-L.; Yuan, D.-J. Characteristics of dewatering induced drawdown curve under blocking effect of retaining wall in aquifer. *J. Hydrol.* **2016**, *2016*, 554–566. [CrossRef]
17. Luo, Z.-J.; Zhang, Y.-Y.; Wu, Y.-X. Finite element numerical simulation of three-dimensional seepage control for deep foundation pit dewatering. *J. Hydrodyn.* **2008**, *20*, 596–602. [CrossRef]
18. Ying, L.; Chen, D.; Xingwang, L. Simplified calculation method of decompression dewatering for deep excavation with suspended waterproof curtain. *Rock Soil Mech.* **2021**, *42*, 862. (In Chinese)
19. Xu, Y.-S.; Shen, S.-L.; Ma, L.; Sun, W.-J.; Yin, Z.-Y. Evaluation of the blocking effect of retaining walls on groundwater seepage in aquifers with different insertion depths. *Eng Geol.* **2014**, *183*, 254–264. [CrossRef]
20. Wu, Y.-X.; Shen, S.-L.; Xu, Y.-S.; Yin, Z.-Y. Characteristics of groundwater seepage with cutoff wall in gravel aquifer. I: Field observations. *Can. Geotech. J.* **2015**, *52*, 1526–1538. [CrossRef]
21. Wu, Y.-X.; Shen, S.-L.; Yin, Z.-Y.; Xu, Y.-S. Characteristics of groundwater seepage with cutoff wall in gravel aquifer. II: Numerical analysis. *Can. Geotech. J.* **2015**, *52*, 1539–1549. [CrossRef]
22. Wang, J.-X.; Hu, L.-S.; Wu, L.-G.; Tang, Y.-Q.; Zhu, Y.-F.; Yang, P. Hydraulic barrier function of the underground continuous concrete wall in the pit of subway station and its optimization. *Environ. Geol.* **2009**, *57*, 447–453. [CrossRef]
23. Ministry of Housing and Urban-Rural Development of the People's Republic of China. *Technical Specification for Retaining and Protection of Building Foundation Excavations: JGJ 120—2012*; China Architecture & Building Press: Beijing, China, 2012. (In Chinese)